

A nanoscale demonstration of hydrogen atom spill-
over and surface diffusion across silica using the
kinetics of CO₂ methanation catalyzed on spatially
separate Pt and Co nanoparticles.

*Simon K. Beaumont,^{a,b,c,‡} Selim Alayoglu,^{a,b,‡} Colin Specht,^{a,b} Norbert Kruse,^{d,e} Gabor A.
Somorjai^{a,b,*}*

AUTHOR ADDRESSES ^a Department of Chemistry, University of California, Berkeley, CA

^b Materials Sciences Division, Lawrence Berkeley National Laboratory, Berkeley, CA

^c Department of Chemistry, Durham University, South Road, Durham, DH1 3LE, United
Kingdom

^d Université Libre de Bruxelles, Chimie Physique des Matériaux, Campus de la Plaine CP 243,B-
1050 Bruxelles, Belgium

^e Department of Chemical Engineering and Bioengineering, Washington State University,
Pullman, WA

ABSTRACT Hydrogen spillover is of great importance to understanding many phenomena in heterogeneous catalysis, and has long been controversial. Here we exploit well-defined nanoparticles to demonstrate its occurrence through evaluation of CO₂ methanation kinetics. Combining platinum and cobalt nanoparticles causes a substantial increase in reaction rate; but increasing the spatial separation between discrete cobalt and platinum entities results in a dramatic ~50% drop in apparent activation energy, symptomatic of H-atom surface diffusion limiting the reaction rate.

KEYWORDS

Hydrogen spillover, nanoparticles, catalysis, surface diffusion, transport limited, CO₂ methanation.

TEXT Hydrogen spillover onto catalyst support materials – defined as the net migration of hydrogen atoms from a hydrogen-rich metal surface onto a hydrogen-poor metal oxide support – has been a controversial topic in heterogeneous catalysis since its first identification for a platinum catalyst in contact with WO₃ in 1964.¹ It is a topic which has been reviewed well elsewhere² – and most recently by Prins.³ It is a topic of tremendous importance in understanding the molecular level mode of operation of heterogeneous catalysts where hydrogenation or dehydrogenation occurs – a grouping that includes many of the world’s major chemical processes.

Hydrogen spillover onto reducible oxides (WO₃, CeO₂ etc.) is a widely accepted process and we have recently demonstrated using in situ diffraction that it can dramatically expand the lattice size of CeO₂ when hydrogen spills over from Pt to CeO₂, causing reduction of the oxide (Ce³⁺ is substantially larger in size than Ce⁴⁺).⁴ In contrast, there is very little incontrovertible evidence

for H₂ spillover occurring on non-reducible metal oxides, in particular Al₂O₃ and SiO₂, which are commonly used to support metal particles in heterogeneous catalysis.³ This is because, while reducible oxides can transfer protons and electrons independently by reduction of the support (and thus allow a net migration of hydrogen atoms as proton plus electron), there is no low energy pathway thought to exist for H atoms to interact with irreducible supports. Molecular orbital energy calculations have been conducted on materials such as low index surfaces of Al₂O₃ and SiO₂ showing H-atom spillover to be unfavorable.^{5,6} Many examples of alleged hydrogen spillover on these materials have been reported, but it is argued there are simpler explanations such as migration of other reactants to the metal site,⁷ contamination of the catalysts⁸ or migration of the metal itself across the support.⁹ In many cases H-D exchange has been claimed to indicate H atom spillover, but it is important to note that the minimum necessary criterion for H-D exchange on the support is only that H⁺ and D⁺ ions can interchange (with no net H-atom transfer). For hydrogenation reactions the distinction between net hydrogen atom transfer (leading to the possibility of increased hydrogenation rates) and proton exchange is, however, an important one.

We have recently conducted work on platinum and cobalt nanoparticles as heterogeneous catalysts for Fischer-Tropsch and CO₂ hydrogenation, because precious metals including Pt are known to promote these important reactions, but their exact role remains subject to debate. When starting with CO₂ as a reactant two products dominate, CO (Reverse Water Gas Shift, RWGS) and CH₄ (methanation).¹⁰ On identifying that bimetallic CoPt nanoparticles initially prepared as a homogeneous alloy, underwent Pt surface-segregation in reducing atmospheres, and were thus not capable of CO₂ methanation,¹¹ we have moved to look at individual Pt nanoparticles and Co nanoparticles as an improved model for such catalysts. With both Pt and Co monometallic

nanoparticles deposited nearby to one another, we measured a promotional effect in catalytic methanation reactions and identified (using in situ X-ray spectroscopy in H₂) that nearby Pt nanoparticles were able to enhance the reduction of Co nanoparticles deposited within the same film (for a film of only one nanoparticle depth).¹² We therefore proposed that hydrogen atom transfer seen to be occurring during in situ reduction monitored by NEXAFS was also enhancing the rate of reaction by removing surface oxide that is formed when CO₂ dissociates on the cobalt surface (See Figure 1(a)). The stepwise process in which Pt nanoparticles dissociate hydrogen and it then migrates as H-atoms to cobalt nanoparticles, where the CO₂ reduction to methane can occur, offers an excellent tool for exploring hydrogen atom migration (we have previously shown pure Pt does not produce any methane¹¹). In the present study we investigate the effect on the reaction kinetics of increasing the spacing between the Pt and the Co nanoparticles. The decrease of the apparent activation energy to approximately half its value on pure Co when the distance between Pt and Co particles is large suggests diffusion limitation is occurring in the latter case. We attribute this to the diffusion limited migration of hydrogen atoms from Pt to Co nanoparticles.

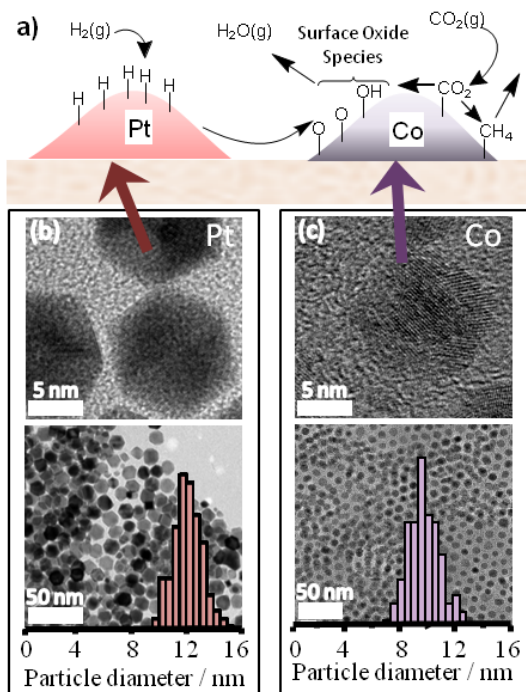


Figure 1. (a) Schematic showing possible pathway for platinum nanoparticle to enhance rate of CO₂ hydrogenation over nearby cobalt nanoparticles via: (1) dissociative chemisorption of hydrogen on platinum; (2) hydrogen spillover from Pt across SiO₂ to Co; and (3) enhanced rate of reaction with proposed surface oxide species generated from the dissociation of CO₂. (b) Transmission electron micrographs of ~ 12 nm platinum nanoparticles, with size distribution overlay of lower image. (c) Transmission electron micrographs of ~ 10 nm cobalt nanoparticles, with size distribution overlay of lower image.

Figure 1 (b and c) show transmission electron micrographs of the as prepared nanoparticles of Pt and Co respectively, which were used to prepare all catalysts in this study, along with their respective size distributions, showing the Co particle diameters are 10 ± 1 nm and the Pt are 12 ± 1 nm and so for our purposes are similar in size. Typical micrographs of the supported catalysts are shown in Figure 2 for the case of Pt and Co nanoparticles mixed in solution and then deposited within MCF-17 mesoporous silica. As can be seen by the lack of nanoparticles concentrated at the edges of the silica, the nanoparticles are deposited inside the pores of MCF-17 mesoporous silica (with pore sizes in the characteristic range of 20–50 nm), which is

deliberately selected to accommodate the relatively large nanoparticles (9 - 13 nm). Samples before (a) and after (b) reaction suggest the individual particles are not substantially changed by the reaction. The change in average particle size is smaller than the width of the distribution (see supporting information). It should be noted that the majority of the particles are expected to be cobalt particles (Co:Pt particle ratio $\sim 24:1$ based on ICP-AES), and the density of particles in the bright field images appears visually comparable with pure cobalt samples of similar loadings reported previously.¹³

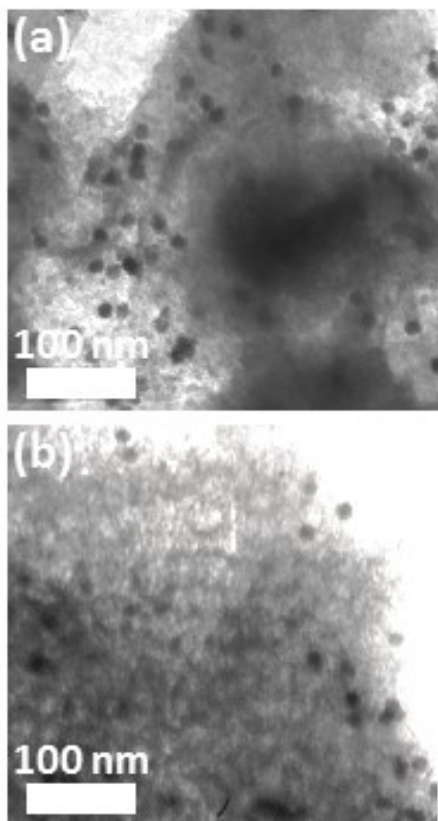


Figure 2. (a) before catalysis and (b) after catalysis: typical bright field transmission electron micrographs of ~ 12 nm platinum nanoparticles and ~ 10 nm cobalt nanoparticles mixed as a colloidal solution and deposited in MCF-17, indicating a general preservation of particle size compared to the unsupported particles shown in Figure 1. Images are artificially processed to brighten / maximize contrast.

For Pt, use of STEM EDS (Scanning Transmission Electron Microscopy Energy Dispersive Spectroscopy), Figure 3 (a), shows identifiable distinct particles of the correct size embedded within the silica matrix. For Cobalt, although it is clearly present, the higher concentrations and lower contrast (as seen by comparison to the dark field image in Figure 2 (b)) mean that the Co cannot readily be identified as discrete particles using the STEM EDS technique when probing through these thick 3D materials (as required to identify discrete Pt particles). Confirmation of the expected cobalt to platinum ratios is arrived at instead by dissolution of the metal phase in aqua regia and the subsequent ICP-AES analysis as presented in Table 1. Table 1 shows four catalysts: (1) pure Pt nanoparticles only; (2) pure Co nanoparticles only; (3) Co nanoparticles and Pt nanoparticles mixed as colloidal solutions and subsequently deposited in MCF-17; and (4) Co/MCF-17 and Pt/MFC-17 deposited and prepared as separate catalysts and then mechanically mixed as powders. The anticipated result of mixing Co and Pt nanoparticles in this manner is shown schematically in the table.

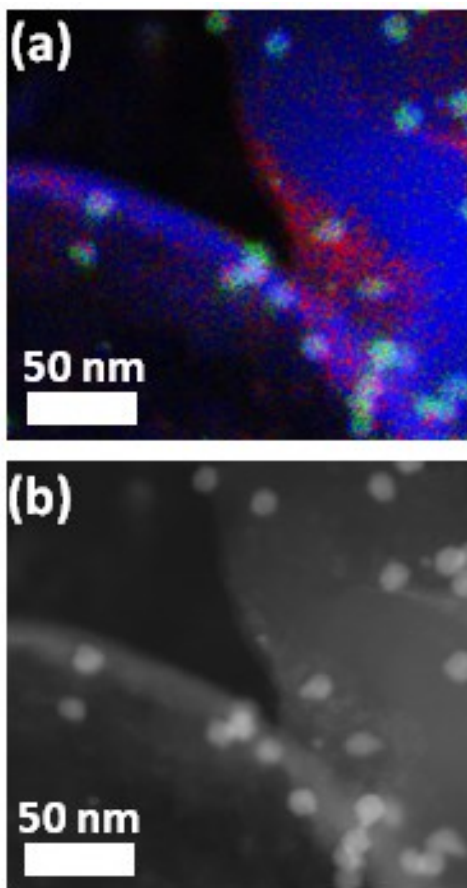
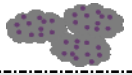
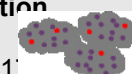
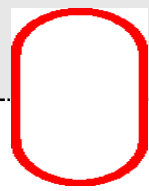
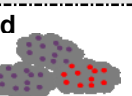


Figure 3. (a) STEM EDS map of the same sample as in Figure 2 (~ 12 nm platinum nanoparticles and ~ 10 nm nanoparticles mixed as a colloidal solution and deposited in MCF-17), but showing Co(red); Pt (green); and silicon (blue) – see discussion in text. (b) Dark field image of the same region as in (a), bright objects likely correspond to Pt as this has higher contrast.

Table 1. Showing composition (determined by ICP-AES); reaction conversion for the production of CO and methane during catalytic CO₂ reduction for a series of MCF-17 supported nanoparticle catalysts.^a

Catalyst ^b	wt% Co (ICP)	wt% Pt (ICP)	Molar ratio Pt/Co	Conversion of CO ₂ to CO product / % ^c	Conversion of CO ₂ to CH ₄ product / % ^c	CO ₂ methanation turnover frequency ^d
Pure Platinum Pt MCF-17 	0	1.1	n/a	0.98	<0.05	n/a
Pure Cobalt Co MCF-17 	4.9	0.0	n/a	2.1	3.0	89 ± 4
Colloidal Solution Mixed [Pt + Co]/MCF-17 	4.0	0.7	0.05	3.1	7.4	
Powders Mixed Pt/MCF-17 + Co/MCF-17 	3.0	0.4	0.04	2.5	5.4	

^aReaction conditions: 1:3:0.5 CO₂ : H₂ : He at 250 °C and 6 bar total pressure. Comparable data obtained at 1 bar total pressure are given in the supporting information. ^bAll catalysts comprise ~12 nm platinum and/or ~10 nm cobalt nanoparticles (as shown in Figure 1) deposited in the pores of mesoporous (MCF-17) silica. Schematics of catalysts indicate approximate proximity of Co (purple) and Pt (red) on MCF-17 granules (grey) as a result of the powder or colloidal solution mixing procedures described in the experimental methodology. ^cConversion to a specified product as a % of total CO₂ available for reaction. ^dTurnover frequency in CH₄ molecules produced per surface Co atom per hour, calculated as described in the supporting information.

Firstly, it can be clearly seen that the turnover frequencies (per surface cobalt atom) in Table 1 indicate there is a significant enhancement on the rate of methane production (3-4 times) when only small numbers of Pt particles are added (circled numbers). This is true whether prepared by mixing the Pt and Co as silica supported powders or mixing at the colloidal solution stage. In contrast, the production of CO does not vary markedly – an interesting observation as it suggests that the two mechanisms (RWGS and methanation) are not directly coupled in CO₂ reduction. Consistent with this, only traces of higher molecular weight products are seen (expected under

these conditions for CO and H₂ reacting, suggesting that CH₄ is formed directly and is not a secondary product resulting from re-adsorption).

It is also worthwhile noting that the pure platinum nanoparticles produce no detectable methane and even after accounting for the metal loading and nanoparticle size, produce only slightly more CO than their cobalt analogues. Accordingly, the enhanced rates of methanation in the presence of small (<5%) numbers of platinum particles is not the result of platinum increasing the carbon monoxide concentration (secondary reactions) or of producing methane directly.

Although the numbers in Table 1 suggest there is little difference in the enhancement as a result of colloidal solution or powder mixing this is not the case as the temperature is varied. Figure 4 shows a summary of the activation energies obtained from a series of Arrhenius plots for production of both CO and CH₄ (given in supporting information). It should also be noted that comparable data is obtained at 1 bar as shown in the supporting information, indicating the results obtained are not unique to the particular pressure at which the experiment was conducted.

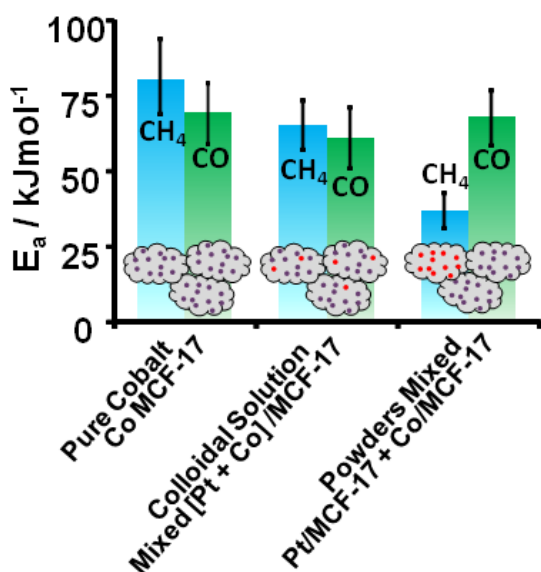


Figure 4. Summary of apparent activation energies from Arrhenius plots (supporting information) at 6 bar total pressure and 200 - 300 °C. Apparent activation energies are shown for

both the production rate of CO (green) and CH₄ (blue) during catalytic CO₂ reduction (1:3:0.5 CO₂: H₂ : He) at 200 - 300 °C. As before, schematics of catalysts indicate approximate proximity of Co (purple) and Pt (red) on MCF-17 granules (grey). Error bars indicated represent uncertainty based on minimum and maximum possible gradients in Arrhenius plots.

As can be seen from Figure 4, the observed activation energy for CO₂ to CO conversion doesn't vary (within error) and is within the range of values identified for reverse water gas shift reactions over a range of metal catalysts¹⁴ - although these are a source of some debate, owing to questions about the validity of assuming equilibrium conditions apply when deriving them from forward water-gas shift values at very low (non-equilibrium) conversions.¹⁴ While the values for cobalt are very consistent, the value for the pure Pt catalyst (see supporting information) is much lower (~ 25 - 40 kJ mol⁻¹).

In contrast, for CO₂ conversion to CH₄ under the same conditions, there is a dramatic decrease in the apparent activation energy, when comparing the samples containing both cobalt and platinum nanoparticles to the pure Co/MCF-17. On changing from the colloidal solution mixed sample (in which the Pt and Co nanoparticles are anticipated to be randomly distributed within the same MCF-17 granules – i.e. near to one another) to the sample prepared by mixing powders (i.e. where the distance between Pt and Co is the distance between separate MCF-17 entities – roughly 0.4 - 5 μm in size), the apparent activation energy drops even further – to about half the value on pure cobalt. (This compares to distances of up to a couple of hundred nm at most, when both Co and Pt are deposited within the pores of mesoporous silica, as indicated in the supporting information). It should be noted that this drop in apparent activation energy cannot be the consequence of the cobalt acting as a “porthole” for hydrogen adsorbed nearby,¹⁵ since the effect is not observed in the absence of added Pt. The value of ~80 kJ mol⁻¹ obtained on the pure Co sample is consistent with our previous findings on different sizes of Co nanoparticles,¹³ and

values reported for CO₂ methanation over other metals such as Ru and Ni.¹⁶ The values typically obtained even for Ni (usually considered an optimal catalyst for CO₂ methanation) are much higher than the apparent activation energy for the Co and Pt mixed powders sample (> 80 vs. 37 ± 6 kJmol⁻¹). It is therefore unlikely the change observed in the apparent activation energy is the result of true activation energy change, but is instead likely to be due to other effects. (This behavior is replicated in the second data set obtained at 1 bar as shown in the supporting information).

The most likely cause for this marked drop in activation energy is the occurrence of a transport limited process. The presence of diffusion limitations is very well known to have a strong effect on the apparent activation energy that is measured – and indeed when diffusion is important it can even be shown, at least for the case of diffusion in and out of idealised spherical particles, that diffusion limitations result in the $E_a^{\text{apparent}} \approx \Delta E_a/2$.^{17,18} This is consistent with the diffusion limitations becoming steadily more pronounced (E_a^{apparent} lower) in the different catalysts from pure Co, where all the chemistry occurs on a single nanoparticle, to the mixed powders, where hydrogen is diffusing following dissociative chemisorption on Pt in one MCF-17 granule to cobalt nanoparticle in an adjacent silica granule – presumably via contact points of the two silica granules. The limited availability of such contact points may contribute to the diffusion limitation occurring. It should be noted this is accompanied by the observation of a so called ‘compensation effect’ as detailed in the supporting information.¹⁸

The results presented above are strongly indicative of a reaction mechanism involving net hydrogen atom migration. However, it should be noticed in the present case that the proposed mechanism requires only H atom migration across support sites. This is a key difference to many previous studies,³ where attempts have been made to identify hydrogen spillover by looking for

a population of atomic hydrogen on the support or long enough lived spillover hydrogen atoms to have time to react at low density support sites. While the arguments put forward that unfavorable energy cost of hydrogen atom spillover to non-reducible supports would prohibit its occurrence, this only holds for obtaining a significant fraction of the total hydrogen atom population on the support and not for temporary thermally activated migration. Silica is a non-reducible support and so H-atom migration cannot occur via reduction and separate transfer of a proton and an electron – a process that further complicates the picture when reducible materials such as CeO₂ or TiO₂ are used as supports – a topic that may be interesting to explore in future studies.

It could potentially be argued that the reason for this phenomenon being observed here is due to hydrocarbon contaminants migrating away from the active metal on dilution with a second catalyst support material, as was observed with the addition of alumina to Pt/SiO₂ used in ethylene hydrogenation, and initially incorrectly ascribed to hydrogen spillover.⁸ However, this fails to offer a good explanation for the drop in activation energies above being precisely what would be expected for a diffusion limited process (and the absence of a rate difference at higher temperatures). Migration of hydrocarbon contaminants is also not consistent with the only slight decrease in total cobalt metal loading on the more active catalysts (rather than the dramatic increase in support material for the case described above).

In summary, preparation of Co-Pt catalysts using both individual size controlled Pt nanoparticles and Co nanoparticles rather than bimetallic particles results in a turnover rate enhancement for CO₂ methanation of ×3 versus the pure cobalt nanoparticles at low temperatures (typical of Fischer-Tropsch catalysis in which Pt promoted Co catalysts are commonly employed). This holds true whether deposited within the pores of a single sample of mesoporous

silica, or separate batches of mesoporous silica which are subsequently mixed together. Arrhenius plots for CO₂ methanation by the different catalysts indicate a dramatic drop in apparent activation energy as Pt is introduced; an effect that becomes more pronounced when the average Pt to Co distance is increased. This implies the reaction becomes transport limited by introducing the Pt nanoparticles as a promoter. We suggest the origin for this is that dissociated hydrogen atoms migrate across the silica surface to reduce surface oxide formed on the cobalt by the CO₂ dissociation step in the reaction. This suggests hydrogen spillover onto a non-reducible silica support, while it may not give rise to large populations of H-atoms on the support, can effect the migration of dissociated H-atoms between metal objects some distance apart from each other on a catalyst's surface, and therefore has an important role to play in heterogeneous catalysis.

Supporting Information. Experimental methods including nanoparticle synthesis; Arrhenius plots; additional data obtained at 1 bar total pressure; compensation effect data; estimation of interparticle distance. This material is available free of charge via the Internet at <http://pubs.acs.org>.

Corresponding Author

*GAS Tel: (510) 642-4053 E-mail:somorjai@berkeley.edu

Notes

The authors declare no competing financial interests.

Author Contributions

The manuscript was written through contributions of all authors. All authors have given approval to the final version of the manuscript. ‡These authors contributed equally.

ACKNOWLEDGMENT

This work was supported by the Director, Office of Basic Energy Sciences, Materials Science and Engineering Division and the Division of Chemical Sciences, Geological and Biosciences of the U.S. Department of Energy under Contract No. DE-AC02-05CH11231. SKB and NK gratefully acknowledge financial support by Total S.A. We are also thankful for valuable discussions with Daniel Curulla-Ferre (Total S.A.).

REFERENCES

- ¹ Khoobiar, S. *J. Phys. Chem.* **1964**, *68*, 411-412.
- ² Conner, W. C.; Falconer, J. L. *Chem. Rev. (Washington, DC, U. S.)* **1995**, *95*, 759-788.
- ³ Prins, R. *Chem. Rev. (Washington, DC, U. S.)* **2012**, *112*, 2714.
- ⁴ Alayoglu, S.; An, K. J.; Melaet, G.; Chen, S. Y.; Bernardi, F.; Wang, L. W.; Lindeman, A. E.; Musselwhite, N.; Guo, J. H.; Liu, Z.; Marcus, M. A.; Somorjai, G. A. *J. Phys. Chem. C* **2013**, *117*, 26608-26616.
- ⁵ Karna, S. P.; Pugh, R. D.; Shedd, W. M.; Singaraju, B. B. K. *J. Non-Cryst. Solids* **1999**, *254*, 66-73.
- ⁶ Ahmed, F.; Alam, M. K.; Suzuki, A.; Koyama, M.; Tsuboi, H.; Hatakeyama, N.; Endou, A.; Takaba, H.; Del Carpio, C. A.; Kubo, M.; Miyamoto, A. *J. Phys. Chem. C* **2009**, *113*, 15676-15683.
- ⁷ Ueda, R.; Kusakari, T.; Tomishige, K.; Fujimoto, K. *J. Catal.* **2000**, *194*, 14-22.

- ⁸ Schlatter, J. C.; Boudart, M. *J. Catal.* **1972**, *24*, 482-492.
- ⁹ Liu, H. Y.; Chiou, W. A.; Fröhlich, G.; Sachtler, W. H. *Top. Catal.* **2000**, *10*, 49-57.
- ¹⁰ It should be noted that although RWGS is an equilibrium reaction we are operating in H₂ rich, low conversion conditions where this is not anticipated to be important.
- ¹¹ Alayoglu, S.; Beaumont, S. K.; Zheng, F.; Pushkarev, V. V.; Zheng, H. M.; Iablokov, V.; Liu, Z.; Guo, J. H.; Kruse, N.; Somorjai, G. A. *Top. Catal.* **2011**, *54*, 778-785.
- ¹² Beaumont, S.K.; Alayoglu, S.; Specht C.; Michalak, W.D.; Pushkarev, V.V.; Guo, J.; Kruse N. and Somorjai, G.A., *J. Am. Chem. Soc.* **2014**, *136*, 9898-9901.
- ¹³ Iablokov, V.; Beaumont, S. K.; Alayoglu, S.; Pushkarev, V. V.; Specht, C.; Gao, J. H.; Alivisatos, A. P.; Kruse, N.; Somorjai, G. A. *Nano Lett.* **2012**, *12*, 3091-3096.
- ¹⁴ Spencer, M. S. *Catal. Lett.* **1995**, *32*, 9-13.
- ¹⁵ Taylor, H. *Annu. Rev. Phys. Chem.* **1961**, *12*, 127-150.
- ¹⁶ Wei, W.; Jinlong, G. *Front. Chem. Sci. Eng.* **2011**, *5*, 2-10.
- ¹⁷ Chorkendorff, I.; Niemantsverdriet, J. W. *Concepts of Modern Catalysis and Kinetics*; 2nd ed.; Wiley-VCH: Weinheim, **2007**.
- ¹⁸ Boudart, M.; Djéga-Mariadassou, G. *Kinetics of Heterogeneous Catalytic Reactions*; 1st ed.; Princeton University Press: Princeton, **1984**.

TOC GRAPHIC:

